HHS Public Access

Author manuscript

Biomaterials. Author manuscript; available in PMC 2016 December 01.

Published in final edited form as:

Biomaterials. 2015 December ; 72: 11–19. doi:10.1016/j.biomaterials.2015.08.041.

Enhancing neural stem cell response to SDF-1α gradients through hyaluronic acid-laminin hydrogels

CP Addington[1], **JM Heffernan**[1,2], **CS Millar-Haskell**[1], **EW Tucker**[1], **RW Sirianni**[1,2], and **SE Stabenfeldt**[1,*]

[1]School of Biological and Health Systems Engineering, Arizona State University, Tempe, AZ, USA

[2]Barrow Brain Tumor Research Center, Barrow Neurological Institute, Phoenix, AZ, USA

Abstract

Traumatic brain injury (TBI) initiates an expansive biochemical insult that is largely responsible for the long-term dysfunction associated with TBI; however, current clinical treatments fall short of addressing these underlying sequelae. Pre-clinical investigations have used stem cell transplantation with moderate success, plagued by staggeringly low survival and engraftment rates (2–4%). As such, providing cell transplants with the means to better dynamically respond to injury-related signals within the transplant microenvironment may afford improved transplantation survival and engraftment rates. The chemokine stromal cell-derived factor-1α (SDF-1α) is a potent chemotactic signal that is readily present after TBI. In this study, we sought to develop a transplantation vehicle to ultimately enhance the responsiveness of neural transplants to injury-induced SDF-1α. Specifically, we hypothesize that a hyaluronic acid (HA) and laminin (Lm) hydrogel would promote 1. upregulated expression of the SDF-1α receptor CXCR4 in neural progenitor/stem cells (NPSCs) and 2. NPSC migration in response to SDF-1α gradients. We demonstrated successful development of a HA-Lm hydrogel and utilized standard protein and cellular assays to probe NPSC CXCR4 expression and NPSC chemotactic migration. The findings demonstrated that NPSCs significantly increased CXCR4 expression after 48 hrs of culture on the HA-Lm gel in a manner critically dependent on both HA and laminin. Moreover, the HA-Lm hydrogel significantly increased NPSC chemotactic migration in response to SDF-1α at 48 hrs, an effect that was critically dependent on HA, laminin and the SDF-1α gradient. Therefore, this hydrogel serves to 1. prime NPSCs for the injury microenvironment and 2. provide the appropriate infrastructure to support migration into the surrounding tissue, equipping cells with the tools to more effectively respond to the injury microenvironment.

Corresponding Author: Sarah Stabenfeldt, Tel: 480-965-8336, Fax: 480-727-7624, sarah.stabenfeldt@asu.edu.
Author Postal Addresses:
[1]Arizona State University, School of Biological and Health Systems Engineering, P.O. Box 879709, Tempe, AZ, 85287-9709
[2]Barrow Neurological Institute, Barrow Brain Tumor Research Center, 350 W Thomas Road, Phoenix, AZ 85013

Keywords

chemotaxis; SDF-1α-CXCR4 axis; tissue engineering; brain injury; regenerative medicine

1. Introduction

The impact of traumatic brain injury (TBI) has only recently garnered recognition from many social and healthcare communities despite its long-standing prevalence in the U.S. Approximately 1.7 million people sustain a TBI annually and the costs associated with TBI create a $76.5 billion strain on the American healthcare system and economy [1–3]. Long-term dysfunctions associated with TBI (e.g. chronic traumatic encephalopathy and motor impairment) [4–6] are largely due to the secondary, biochemical injury that follows the primary, mechanical insult; however, no clinical treatments directly target these underlying pathologies associated with TBI. Pre-clinical studies have investigated stem cell transplantation as a means to mitigate the effects of the secondary injury, but have suffered from staggeringly low rates of cell survival and engraftment (2–4%) [7–10]. This major limitation is mainly attributed to the cytotoxic injury microenvironment created by a systemic and neural inflammatory response, which is mediated by inflammatory cells that infiltrate the blood brain barrier and locally activated glia, respectively [11–13]. Activated glia also secrete factors that promote the endogenous repair response including the chemokine stromal cell-derived factor 1α (SDF-1α), which has been shown to play a critical role in recruitment of endogenous neural progenitor/stem cells (NPSCs) to the site of injury [14,15]. Exploiting this endogenous SDF-1α signaling paradigm for exogenous transplant strategies may serve to increase NPSC migration and engraftment into the surrounding tissue following transplantation. As such, we aimed to develop a neurotransplantation platform that promotes exogenous cell response to injury-relevant SDF-1α signaling.

Tissue-engineered constructs have been used previously in an attempt to create a permissive transplant microenvironment; often in the form of hydrogels as their mechanical and cellular adhesion properties are easily tuned to mimic native neural tissue. The extracellular matrix (ECM) of native brain tissue is largely comprised of proteoglycans (e.g. lecticans), hyaluronic acid and tenascin C and R [16,17]. Specifically, the glycosaminoglycan hyaluronic acid (HA) is prominently expressed near neural stem cell niches and neuroblast migration routes (within the subventricular zone and rostral migratory stream, respectively) [18]. HA-based hydrogels are therefore a natural extension into mimicking the native neural ECM, and numerous groups have reported that HA-based hydrogels support survival, differentiation and proliferation of neural cell types *in vitro* and *in vivo* [19–22]. However, the effect of HA on NPSC migration remains largely unexplored despite the knowledge that normal physiological NPSC migration *in vivo* follows an HA-rich route [18]. Given these findings, the benefit of elucidating the relationship between HA and NPSC migration becomes evident.

Recent cell signaling studies have identified crosstalk between HA and the injury-related chemokine SDF-1α in mesenchymal (MSCs) [23] and hematopoietic stem cells (HSCs) [24,25] that resulted in heightened responsiveness to SDF-1α gradients. For example, MSCs

cultured on HA substrate upregulate the SDF-1α receptor CXCR4, indicative of signaling crosstalk between HA and SDF-1α-axes [23]. The probability for similar HA-SDF-1α crosstalk mechanisms to exist in NPSCs is high, as NPSCs inherently express CXCR4 and the primary HA receptor CD44 [26,27]. Previous HA hydrogel platforms for neural tissue engineering considered HA a “blank slate” where tethered protein or peptide-binding motifs serve as the primary cellular interfacing domains. However, we postulate that rather than serving as a “blank slate”, HA will actively contribute to promoting NPSC chemotactic migration through HA-SDF-1α crosstalk.

Knowledge of HA-SDF-1α crosstalk will significantly inform next generation hydrogel systems capable of biochemically priming neurotransplants to dynamically respond to the local injury environment. We acknowledge that HA alone, however, is not sufficient to promote NPSC adhesion and migration effectively [28]. Thus, incorporation of an ECM protein known to support NPSC migration may provide the appropriate infrastructure for NPSCs to respond to SDF-1α gradients. We have previously reported that laminin and SDF-1α work synergistically to increase NPSC migration *in vitro* [29]. Therefore, in this work we have investigated a dual-purpose hydrogel system comprised of both HA (to modulate CXCR4 expression) and laminin (to provide adhesive cues). We hypothesize that HA-laminin hydrogels will 1. increase NPSC responsiveness to SDF-1α gradients and 2. provide a substrate that facilitates NPSC migration in response to injury relevant SDF-1α gradients, thereby equipping NPSCs with tools to dynamically respond to the neural injury environment.

2. Materials and Methods

2.1. Materials for polymer synthesis

3,3 Dithiopropionic acid (DTPA), anhydrous methanol, anhydrous ethanol, hydrazine hydrate (HH), hexane, concentrated sulfuric acid, ethyl ether, hydrochloric acid (HCl), sodium hydroxide (NaOH), sodium chloride (NaCl), hyaluronic acid sodium salt (HA) from Streptococcus equi, N-3-dimethylaminopropyl-N′-ethylcarbodiimide hydrochloride (EDC), 5,5'-dithiobis-2-nitrobenzoic acid (Ellman’s reagent), and laminin-111 were purchased from Sigma Aldrich (St. Louis, MO, USA). Dithiothreitol (DTT) was purchased from Gold Biotechnology (St. Louis, MO, USA). Poly(ethylene glycol) divinyl sulfone (PEGDVS) 5 kDa was purchased from JenKem Technology USA (Allen, TX, USA).

2.2. HA-Lm Gel Formation

Dithiopropionic dihydrazide (DTPH) was synthesized from DTPA and HH in a two-step reaction as previously described [30]. High molecular weight HA was functionalized with thiol groups through conjugation of the terminal hydrazides on DTPH to the carboxyl groups on HA using EDC chemistry and subsequent reduction of disulfide bonds using DTT as previously described [31]. ^{1}H NMR spectra was collected in D_2O (400 MHz Varian liquid state NMR, Agilent Technologies, Santa Clara, CA, USA), and Ellman’s reagent test was used to quantify the concentration of conjugated thiols [32]. HA-S was sterilized by ethylene oxide gas and stored at −20°C.

HA-S hydrogels were formed via Michael-type addition crosslinking with PEGDVS as previously reported [33]. Briefly, PEGDVS was dissolved in media at a concentration that yielded an equimolar ratio of thiol-reactive groups to thiols present on the HA-S. HA-S was dissolved in pH 3 mitogenic growth factor-free culture media (formulation described under section 2.2 NPSC isolation and culture) and titrated between pH 7 and pH 8 with 1 M NaOH using phenol red as a colorimetric indicator of pH. The HA-S solution was mixed with an equal volume of crosslinker solution and vortex mixed for 15 seconds prior to plating.

Laminin was determined to have free thiols available for binding by Ellman's reagent test, presumably from its cysteine-rich β chain (data not shown). Laminin was conjugated to PEGDVS via Michael addition at 0.01 wt% and 0.10 wt% respectively in PBS for 15 minutes at room temperature. The solution was purified by dialysis against Tris-buffered saline to remove unbound PEGDVS and freeze dried. Capacity for covalent immobilization of laminin was evaluated by ^{1}H NMR spectra in D_2O. Spectra were analyzed for ratio of PEG groups to vinyl groups and compared to non-reacted PEGDVS spectra to observe differences in vinyl groups available for binding. Based on data presented in section 3.1, laminin was incorporated within the gel at pre-determined concentrations by mixing with PEGDVS media solution and allowed to react 15 minutes at room temperature prior to mixing with HA-S solution, where PEGDVS concentration was adjusted to account for laminin incorporation.

2.3. NPSC isolation and culture

NPSCs were isolated from the medial and lateral germinal eminences of E14.5 C57BL/6 mice based on previously published protocols [34] and in accordance with a protocol approved by the Institutional Animal Care and Use Committee at Arizona State University. Briefly, mice were anesthetized at 3% isoflurane, rapidly decapitated, and fetuses were extracted from both uterine horns. Fetal tissue was rinsed in cold Leibovitz medium (Life Technologies, Carlsbad, CA) at each stage of the germinal eminence dissection. The germinal eminences were rinsed with sterile, cold Leibovitz medium before mechanical dissociation in working NPSC medium (glucose (6 mg/mL, Acros Organics, Geel, Belgium), HEPES buffer (5mM), progesterone (62.9 ng/mL), putrescine (9.6 μg/mL), heparin (1.83μg/mL), B27 growth supplement (1×, Life Technologies), epidermal growth factor (20 ng/mL), fibroblast growth factor (5 ng/mL), insulin (5 μg/mL), transferrin (5 μg/mL), sodium selenite (5 ng/mL) in Dulbecco's Modified Eagle Medium (Life Technologies), reagents from Sigma Aldrich unless otherwise specified) and plated at a density of 10^4 cells/mL in a humidified incubator at 37°C, 20% O_2, and 5% CO_2. NPSCs were cultured as non-adherent neurospheres in working NPSC medium, passaged by mechanical dissociation, and utilized for experiments between passages 3 through 6.

2.4. NPSC Response to Varied HA-Lm Gel Formulations

Gels were varied in HA and laminin concentration (Table 1) and optimized based on cellular response—i.e. NPSC viability, density and chain formation. HA concentrations (1.75 wt%, 2.00 wt%, 2.25 wt%) were selected based on previously reported rheological data for HA-PEGDVS gels [33] to mimic the stiffness of native neural tissue (0.2–1.0kPa) [35] and on observations that gels below 1.75 wt% HA did not support effective NPSC encapsulation

necessary for transplantation. Laminin concentrations (0%, 0.005%, 0.01%, 0.015%) were selected based on hydrogels in the literature and as an extrapolation of our 2D ECM culture model [29,31,36]. HA-Lm gel films (100 μm thickness) were formed in 24-well plates (occupying approximately 85% of the well bottom) at 37 °C for 15 hours, and single cell NPSC suspensions (2×10^3 cells/well) were seeded directly on top of the gel. NPSCs were incubated for 1 hour to allow for adherence to the HA-Lm gel prior to the addition of 500 μL of mitogenic growth factor-free NPSC media to each well. NPSCs were cultured for 72 hours prior to analysis of viability, density, and chain formation.

2.4.1. Cell Density and Viability—After rinsing HA-Lm gels with sterile phosphate buffered saline, NPSCs were stained with Live/Dead assay (Biotium, Hayward, CA). Live cell counts were used to calculate cell density (cells/cm^2) as a measure of cell attachment to the HA-Lm gel. Fluorescent red (dead) and green (live) channel images (n=6 gels per goup, n=3 ROI per gel) were analyzed for number of positively stained cells using the particle counter plugin for Image J (NIH, Bethesda, MD) and reported as percent viability.

2.4.2. Chain Length—It was observed that gel formulations which supported high cell density and viability also supported the formation of chain-like NPSC assemblies as defined by two or more NPSCs visibility connected by continuous outgrowth in a linear fashion. Therefore, NPSC chain length was measured in MatLab as a tertiary metric for gel formulation optimization after 72 hours of culture on HA-Lm gels. Live cell images (n=6 gels per goup, n=3 ROI per gel) were analyzed for longest linear chain length in each frame.

2.5 Physical Properties of HA-Lm Gel

2.5.1. HA-Lm gel stiffness—Parallel plate rheological measurements were used to determine the storage and loss moduli of HA-Lm gels during gelation (Physica MCR101, Anton Paar, Graz, Austria). Briefly, 500 μL HA-Lm solutions were pipetted onto the fixed plate immediately following mixing and the moving plate was lowered to a height of 0.5mm. The gels were tested at 0.5 % strain with an oscillatory frequency of 1 Hz. The stage was heated to 37°C and maintained within a humid environmental chamber. Storage and loss moduli measurements were taken continuously for 6 hrs.

2.5.2. HA-Lm gel porosity and microstructure—HA-Lm gels (7 mm thickness) were formed in 96 well plates for 15 hours, dehydrated through immersion in a series of ethanol washes and subsequently dried with the Balzers CPD020 critical point dryer (Balzers Union Ltd., Liechtenstein) using liquid carbon dioxide as the transition solvent. Samples were cut open to expose interior microstructures, sputter coated with gold/palladium (60:40) using a Technics Hummer Sputter Coater (Anatech Ltd., Alexandria, VA) and imaged via scanning electron microscopy (SEM) on an XL30 ESEM-FEG (FEI, Hillsboro, OR) with a 5kV beam and spot size of 3. Images were analyzed in Matlab for pore diameter and aspect ratio (n=3 images, 90–120 pores quantified per image).

2.6. NPSC CXCR4 Expression on HA-Lm Gel

2.6.1. Temporal CXCR4 Expression—HA-Lm gel films (Low HA/Moderate Lm, 100 μm thickness) were formed in the bottom of 6 well plates and allowed to gel for 15 hours in

humid conditions at 37°C (n=3). NPSCs were seeded in mitogenic growth factor-free media as single cell suspension (5×10^5 cells/mL) directly on top of the films. NPSCs seeded on poly-L-lysine coating (PLL, 10μg/cm^2, MP Biomedicals, Solon, OH) or maintained in non-adherent conditions served as controls. NPSCs were allowed to adhere for 1 hour prior to taking baseline samples (time 0). After culture for 0, 24, 48 and 72 hours, cells were lysed by mechanical agitation in cold RIPA buffer (Bioworld, Dublin, OH) containing proteinase inhibitor cocktail (50 mM Tris-HCl, 150 mM NaCl, 1 mM EDTA1, % NP-40, 0.5% Sodium Deoxycholate, 0.1% SDS, 0.1% protease inhibitor cocktail (Sigma)). Protein concentration was determined by bicinchoninic acid assay (G-Biosciences, St. Louis, MO) prior to SDS-PAGE electrophoresis in 12% bis-acrylamide gels and western blotting for NPSC CXCR4 expression using β-actin to control for loading variability (rabbit anti-CXCR4, 39 kDa, cat no: 2074, Abcam, Cambridge, England; mouse anti-β-actin, 45 kDa, cat no: 926-42212, LI-COR, Lincoln, NE). The Odyssey Infrared Imaging System (LI-COR) was used to visualize bands stained with appropriate secondary antibodies (donkey anti-rabbit IRDye 800; donkey anti-mouse IRDye 680, LI-COR). Band density was quantified with the Image Studio software (LI-COR), normalized internally to β-actin and externally to non-adherent control culture samples and reported as relative density.

2.6.2. Mechanistic CXCR4 Expression—HA-Lm gels were formed as in the temporal CXCR4 expression experiments. NPSCs (5×10^5 cells/mL) were seeded on HA-Lm gels or on HA only gels. Prior to seeding, NPSCs were either pre-treated with anti-CD44 (100μg/mL) to inhibit HA interactions or its isotype control for 45 minutes at 37°C (rat anti-CD44, Millipore, Darmstadt, Germany; rat IgG1 κ isotype control, BioLegend, San Diego, CA) or received no pre-treatment. NPSCs were cultured for 0 and 48 hours, lysed and analyzed by western blotting for CXCR4 expression as reported for temporal CXCR4 expression experiments (rabbit anti-CXCR4, Abcam; mouse anti-beta actin, LI-COR).

2.7. Chemotactic NPSC Migration

HA-Lm gels (1 mm thickness) were formed at the bottom of 24 well plate 8 μm pore size Transwell inserts (Corning Inc., Corning, NY) and allowed to gel for 15 hours at 37°C in humid conditions (n=3 per group). Groups, as outlined in Table 2, included HA only gels, HA-Lm gels only or HA-Lm gels impregnated with the CXCR4 antagonist AMD3100 (5 μg/mL; Santa Cruz Biotechnology, Santa Cruz, CA), rat anti-CD44 (100 μg/mL; Millipore), or an anti-CD44 isotype control (100 μg/mL; rat IgG1 κ BioLegend). NPSCs were then seeded directly on top of the gels (10^5 cells/mL) and cultured for 24 and 48 hours in mitogenic growth factor-free media. NPSCs seeded onto impregnated gels were incubated with their respective supplementation at the appropriate concentration for 45 minutes at 37 °C prior to seeding. As described in Table 2, HA-only or HA-Lm gels were exposed to no SDF-1α, uniform SDF-1α or a gradient of SDF-1α. Uniform SDF-1α gels were allowed to saturate with SDF-1α (1 μg/mL; PeproTech Inc., Rocky Hill, NJ) prior to NPSC seeding and supplemented with 1 μg/mL SDF-1α in both the top and bottom Transwell chambers, while gradient SDF-1α gels were not pre-saturated and the gradient was maintained out to 48 hours. SDF-1α concentration of 1 μg/mL was determined based on previous studies in NPSCs [29]. Effective SDF-1α gradient maintenance out to 48 hours was validated by enzyme-linked immunosorbent assay (ELISA, Supplementary Figure 2). Briefly, gels were

formed in Transwell inserts and exposed to SDF-1α gradients as in chemotactic experiments for 12, 24 or 48 hours (n=3 per time point). SDF-1α concentration of both the lower chamber (donor) and upper chamber (receptor) of the Transwell insert (Supplementary Figure 2) were determined by ELISA. At 24 and 48 hours, NPSCs that had migrated through the gel to the Transwell membrane were stained with DAPI and counted using the cell counter ImageJ plugin (NIH, Bethesda, MD).

2.8 Statistical Analysis

Two-way ANOVA with Tukey's post hoc test was performed for all experiments where statistical analysis was used (NPSC density, viability, chain length, temporal CXCR4 expression and mechanistic CXCR4 expression), where $\alpha=0.05$ in Prism 6 (GraphPad, Inc., La Jolla, CA).

3. Results

3.1. Formation of HA-Lm Gel Components

Successful thiolation of HA was evidenced by the appearance of thiol peaks (2.5 and 2.7 ppm) in the ^{1}H NMR spectrum of HA-S compared to that of HA prior to thiolation (Figure 1A). Moreover, covalent immobilization of laminin to PEG-DVS was apparent through both the appearance of peptide peaks in the NMR spectrum of PEG-DVS (Figure 1B) and the reduction of free vinyl groups relative to PEG groups in PEG-DVS (Figure 1C). Collectively, these data indicate that our methods for formulating HA-Lm gel components enable the covalent immobilization of laminin within an HA hydrogel.

3.2. NPSCs Survive and Spread on HA-Lm Gels at 72 hours

NPSC density after 72 hours of culture on HA-Lm gels was found to be significantly higher on gels with lower HA concentrations and higher laminin concentrations (Low HA/ Moderate and High Lm) compared to all other groups, as illustrated in Figure 2A and Supplementary Figure 1 ($p<0.0001$). Moreover, Low HA/ Moderate and High Lm gels were the only gels to support NPSC density increase above the initial plating density (Figure 2A). In quantifying percent viability, groups with low cell density yielded high variance in percent viability; therefore, groups with a coefficient of variance above 30% were omitted from statistical analysis (omitted groups included High HA gels and No Lm gels). NPSC viability was significantly higher on gels with lower HA concentrations and higher Lm concentrations (Low HA/Moderate and High Lm) compared to all other groups ($p=0.0177$, 0.0026, respectively). Moreover, NPSC chain length was significantly higher on gels that supported high NPSC density and viability (Low HA/ Moderate and High Lm) as compared to all other groups ($p<0.0001$) and on Moderate HA/ High Lm gels compared to all other Moderate HA gels ($p=0.0016$; Figure 3). Overall, Low HA/Moderate and High Lm gels supported the highest NPSC density and viability and longest NPSC chain length. The Low HA/Moderate Lm gel formulation was chosen for subsequent experimentation to minimize laminin reagent consumption.

3.3. HA-Lm Gel Physical Properties are Relevant to Native Neural Tissue

The storage modulus of HA-Lm gels (Low HA/Moderate Lm) was measured as 1.02 kPa by rheology after gelation for 6 hours (G', Figure 4A), which mimics the stiffness of native neural tissue (0.2–1kPa) [35]. Gelation time was 24 minutes at 37°C in humid conditions as indicated by the increase in storage modulus over the loss modulus (Figure 4A). SEM images illustrated a highly porous microstructure within the HA-Lm gel with pore size ranging from 2–17 μm and an average aspect ratio of 2.12 (Figure 4B), providing appropriate porosity for cellular infiltration.

3.4. HA-Lm Gel Upregulates NPSC CXCR4 Protein Expression

NPSC CXCR4 expression was significantly increased after 48 hours of culture on HA-Lm gel compared to NPSCs cultured on poly-L-lysine (PLL) at all time points ($p=0.0408$) and to NPSCs cultured on HA-Lm gel for 24 ($p=0.0145$) and 72 hours ($p=0.0097$). After 72 hours of culture, CXCR4 expression on HA-Lm gel returned to basal PLL CXCR4 expression levels (Figure 5). The significant increase in CXCR4 expression observed at 48 hours on HA-Lm gel was abrogated by inhibiting HA interactions with anti-CD44 (Figure 6A,B). CXCR4 expression after 48 hours of culture on HA-Lm gel impregnated with anti-CD44 was significantly reduced compared to that on HA-Lm gel without supplementation ($p<0.0001$) and was not significantly different from CXCR4 expression on PLL at 48 hours (Figure 6B). Moreover, this reduction was due to HA interaction inhibition and not simply to antibody supplementation as CXCR4 expression on gels impregnated with anti-CD44 isotype control was not significantly different from that on HA-Lm gels without supplementation (Figure 6B). NPSC adherence, and subsequently cell lysate protein concentration, was too low on HA only gels to allow for visualization of CXCR4 expression by western blotting.

3.5. HA-Lm Gel Promotes NPSC Chemotactic Migration in Response to SDF-1α Gradients

The Transwell culture set-up successfully maintained an SDF-1α concentration gradient throughout the experiment, as determined by ELISA. After 48 hours, the SDF-1α concentration in the donor (lower chamber) was 1.6-fold higher than that in the receptor (upper chamber) (Supplementary Figure 2). Correspondingly, NPSC migration in response to SDF-1α gradient was significantly increased at 48 hours when compared either to 24 hours of migration in a gradient, or to any time point in response to uniform SDF-1α concentration or no SDF-1α (Figure 7A–C,J; $p=0.0067$, <0.0001 respectively). A 3.8-fold increase in migration over uniform and no SDF-1α was also observed at 24 hours, however it was not significant ($p=0.0676$). Moreover, SDF-1α gradients play a critical role in mediating this response as evidenced by the reduction of NPSC migration to basal levels with the addition of the CXCR4 antagonist AMD3100 (Figure 7D,H). The addition of AMD3100 significantly reduced NPSC migration compared to HA-Lm gels without AMD3100 at both 24 and 48 hours (Figure 7J, $p=0.0299$, <0.0001 respectively). Conversely, NPSC migration in HA-Lm gels+AMD3100 was not significantly different from uniform and no SDF-1α groups at either 24 or 48 hours.

3.6. Enhanced NPSC Chemotactic Response in HA-Lm Gel Requires both HA and Lm

NPSC chemotactic migration was attenuated when laminin was excluded from the gel and abrogated when HA interactions were blocked with an antibody against HA receptor CD44 (Figure 8). At both 24 and 48 hours, NPSC chemotactic migration was significantly reduced on HA-only gels compared to HA-Lm gels ($p=.0085$, <0.0001 respectively). Interestingly, in HA-only gels NPSC migration at 48 hours increased 4.7-fold over that at 24 hours, although the difference was not statistically significant. While a low level of chemotactic migration was preserved in the absence of laminin, inhibiting HA interactions with anti-CD44 abrogated NPSC chemotactic migration such that it was 10- and 8-fold less than NPSC chemotactic migration on HA-Lm gels at 24 and 48 hours, respectively. This significant decrease in NPSC migration in HA-Lm+anti-CD44 gels compared to HA-Lm gels at 24 and 48 hours ($p=0.0046$, <0.0001 respectively) was specifically due to HA interaction inhibition rather than to antibody supplementation as the isotype control for anti-CD44 did not affect NPSC migration.

4. Discussion

Historically, neural progenitor/stem cell (NPSC) transplantation following TBI has been plagued by low survival rates (2–4%) and poor engraftment into the surrounding tissue, which has impeded the full realization of NPSC transplant potential as a therapeutic intervention following TBI [8,37,38]. Some groups have turned to tissue engineered scaffolding to improve cell transplant survival and engraftment following TBI [39–41], while others have primed transplants biochemically for the injury microenvironment (i.e. CXCR4-overexpressing transplants) and observed increased viability and engraftment in the surrounding tissue [42,43]. While both approaches have yielded moderate improvements in transplant survival and engraftment, a dual-purpose hydrogel that simultaneously primes NPSC transplants for the injury microenvironment and provides the appropriate ECM infrastructure could offer the benefits of a multi-component transplant system while minimizing complexity.

Neural tissue engineered scaffolds have largely focused on mimicking the neural niche environment so as to provide cell transplants with an environment permissive to NPSC survival and engraftment. The mechanical properties of the niche are most often re-created in hydrogels for neural tissue engineering as they can be tuned to mimic the stiffness of native neural tissue. Our HA-Lm gel has mechanical properties similar to the neural niche (1.02 kPa storage modulus [35], Figure 4), providing the appropriate mechanical cues to NPSCs. This point is reflected in the significantly higher NPSC viability and density observed on low HA gels compared to moderate and high HA gels (Figure 2). Given that HA content correlates with gel stiffness [33], it can be postulated that the mechanical properties of the low HA gels are better suited for maintenance of NPSC culture than those of the higher HA content gels. However, the niche provides more than just mechanical cues to its resident NPSCs; it also provides critical ECM and soluble signals.

Others have looked at incorporating peptide binding motifs (i.e. RGD or laminin binding domain [21,28]) and ECM proteins (i.e. fibronectin, collagen I, laminin [39,44–46]) within hydrogels to promote cell adhesion, however peptide binding motifs may not fully capture

the functionality of the ECM protein they are intended to mimic and fibronectin and collagen I are not native to neural tissue. The vascular basement membrane protein laminin provides relevant ECM signaling to NPSCs in the subventricular niche where endogenous NPSCs have been shown to leave and home to the site of injury by way of the surrounding vasculature [47,48]. In our system, the inclusion of laminin significantly increased NPSC density, viability and chain formation compared to HA gels without laminin (Figures 2 and 3). Moreover, we have previously observed that signaling crosstalk between laminin and SDF-1α synergistically increases NPSC chemotactic migration [29]. Collectively, these data illustrate the significant role that laminin plays in regulating NPSC migratory behaviors in response to injury-relevant signaling.

Laminin alone does not comprise the niche and, as such, will not fully recapitulate the niche ECM environment for NPSC transplants. Within the subventricular niche, the glycosaminoglycan hyaluronic acid (HA) has been found at higher concentrations than elsewhere in the adult brain [18,49]. Interestingly, evidence of signaling crosstalk between the HA receptor CD44 and laminin was observed by Deboux et al., in which CD44-overexpressing NPSCs plated on laminin were observed to increase spreading and outgrowth [50], suggesting that the roles of laminin and HA in regulating NPSC fate within the niche environment may be more interconnected than previously described. Our data illustrate the critical individual roles that laminin and HA play in providing NPSCs with a substrate to support adherence and migration (laminin) and a substrate to regulate the NPSC receptor expression profile (HA). Upon inhibiting HA interactions, NPSCs remained adhered to the HA-Lm gel but their CXCR4 protein expression was significantly attenuated whereas excluding laminin abrogated NPSC adherence, leaving the system irrelevant for transplantation applications (Figure 5). CXCR4 protein expression within the adult brain is restricted to NPSCs, as such, maintenance of this phenotypic marker without compromising NPSC adhesion and migration may be attributed to the specialized microenvironment of the niche [51]. Therefore, we postulate that the ECM signals provided to NPSCs by the HA-Lm gel are more comprehensive in their recapitulation of the niche ECM environment than previously developed hydrogel systems.

Increases in CXCR4 protein expression on the HA-Lm gel directly correlated with increased NPSC chemotactic migration in response to gradients of the injury-relevant chemokine SDF-1α. Inhibiting NPSC interaction with either component of the gel significantly reduced chemotactic migration in response to SDF-1α gradients indicating the synergistic effect that HA and laminin have on promoting NPSC chemotactic response to SDF-1α (Figure 8). Previous studies on NPSC migration in response to SDF-1α gradients when plated on laminin in 2D yielded data similar to that observed here for HA-Lm gels impregnated with anti-CD44 [29]. Increased NPSC chemotactic migration on HA-Lm gels is critically dependent on SDF-CXCR4 interactions as inhibition of this signaling axis with CXCR4 antagonist AMD3100 reduced NPSC migration to levels comparable to that on HA-Lm gel with either uniform or no SDF-1α (Figure 8); however, it is important to consider alternative mechanisms that may contribute to increased NPSC migration within the HA-Lm gel. CD44 interaction with HA has been observed to precede and facilitate the formation of focal adhesions in other cell types [52,53] and it is thought that CD44 works closely with integrin β1 to promote transmigration of intravenously injected NPSCs as they migrate towards

regions of neural injury [50,54]. Therefore, the role of HA within the HA-Lm gel may not only be to promote CXCR4 expression but also to promote adhesion and migration on laminin. To this end, the results of using of laminin peptide sequences instead of full-length laminin could raise interesting questions regarding the distinct roles of HA and laminin within the gel. Given the mechanistic ambiguity surrounding potential crosstalk between HA and laminin, we feel that the inclusion of full-length laminin may more effectively allow these signaling events to occur. However, future mechanistic studies investigating the distinct role of laminin within the gel may utilize such peptides.

Interestingly, NPSC chemotactic response to SDF-1α was not completely abrogated after 48 hours of culture on HA-only gels (Figure 8). NPSCs cannot form focal adhesions to HA alone as HA interactions are mediated by receptor CD44 and the hyaluronan-mediated motility receptor (RHAMM), not by integrins [55]. Given that NPSC migration in 2D is typically focal adhesion-dependent [56,57], the chemotactic migration of NPSCs within an HA-only gel was a very intriguing finding. Moreover, NPSC adherence to HA only gels in the absence of SDF-1α was minimal (Figure 6), leading us to suspect an interaction between HA and SDF-1α that may alter NPSC adhesion and migration behaviors. We postulate two potential scenarios in which NPSCs may migrate through HA-only gels in the presence of SDF-1α: 1. HA may promote NPSC ECM production and 2. NPSCs may exhibit migratory mode plasticity dependent on environmental conditions. HA has been observed to induce the production of integrin-binding osteopontin and collagens in other cell types [58,59]. Moreover, astrocytes are known to secrete ECM *in vitro* [60] and given the heterogeneous nature of the neurosphere assay [61,62], there may be a subset of NPSCs capable of secreting ECM within the HA only gel. NPSC migration through HA only gels was only observed after 48 hours, thus it is feasible that matrix is being produced on which the NPSCs are then able to migrate in a more typical focal adhesion-mediated manner, however further investigation is necessary to elucidate the potential formation of focal adhesions in this context, particularly in light of low NPSC adherence to HA only gels in the absence of SDF-1α. Alternatively, NPSC migration mechanisms may be more adaptive than previously described as environment-dependent migration mode plasticity has been observed in other cell types (i.e. 2D versus 3D [63,64]). In 3D, cells do not appear to form stable focal adhesions during migration but may instead depend on pseudopodia to move through the ECM [65,66]. Transient cell-matrix and cell-cell adhesion is also found in NPSCs migrating by chain migration mechanisms through the rostral migratory stream (RMS), an area with high concentrations of HA in the adult brain [18]. While chain migration on HA in the RMS draws an interesting conceptual parallel with data presented here, NPSC chain migration has been observed to be dependent on β1 integrin signaling and as such would still require a substrate that supports β1 integrin binding [67]. Interestingly, Avigdor et al. have proposed that SDF-1α may function to increase CD44 avidity to HA in HSCs, allowing for increased HSC retention in SDF-1α rich niches independent of integrin anchoring [25]. Investigating HA-SDF-1α interaction by this mechanism and probing for the formation of focal adhesions in NPSCs migrating on HA-only gels in response to SDF-1α gradients would enlighten these postulations and provide insight into the mechanisms by which NPSCs are migrating in this context.

Regardless of mechanism, the capacity of NPSCs to migrate through the bulk of the HA-Lm gel, as opposed to on top of it or along an interface, indicates the relevancy of the gel to *in vivo* transplantation applications as these cells would be tasked with migration through the bulk of the gel into the surrounding tissue post-transplantation. Thus, NSPC migration through the HA-Lm gel provides motivation for future work investigating its effects after neural injury.

5. Conclusions

Given the local increases in SDF-1α after brain injury and the critical role that others have found SDF-1α to play in regulating NPSC fate after brain injury, increasing NPSC response to SDF-1α may serve as a viable approach to improving NPSC transplant efficacy following TBI. We have shown here that our HA-Lm gel both biochemically primes NPSCs for the injury microenvironment by upregulating the SDF-1α receptor CXCR4 and provides the appropriate ECM cues to promote migration in response to SDF-1α. Therefore, this platform may serve to improve transplant efficacy by providing transplants with the tools to dynamically respond to the injury microenvironment.

Supplementary Material

Refer to Web version on PubMed Central for supplementary material.

Acknowledgements

The authors acknowledge David Lowry and the College of Liberal Arts and Sciences Bioimaging Facility for assistance with electron microscopy, Sanjay Srinivasan for assistance with monomer preparation and the following funding sources: ASU startup funds (SES), NIH 1DP2HD084067 (SES), and ARCS, Inc. Fellowship (CPA), the Barrow Neurological Foundation (JMH, RWS).

References

1. Thurman D, Guerrero J. Trends in hospitalization associated with traumatic brain injury. Journal of Americam Medical Association. 1999; 282:954–957.
2. Coronado VG, McGuire LC, Sarmiento K, Bell J, Lionbarger MR, Jones CD, et al. Trends in Traumatic Brain Injury in the U.S. and the public health response: 1995–2009. Journal of Safety Research. 2012; 43:299–307. [PubMed: 23127680]
3. Arbour RB. Traumatic Brain Injury Pathophysiology, Monitoring, and Mechanism-Based Care. Critical Care Nursing Clinics of North America. 2013; 25:297–319. [PubMed: 23692946]
4. Nolan S. Traumatic brain injury: a review. Critical Care Nursing Quarterly. 2005; 28:188–194. [PubMed: 15875448]
5. McAllister TW. Neurobiological consequences of traumatic brain injury. Dialogues in Clinical Neuroscience. 2011; 13:287. [PubMed: 22033563]
6. McKee AC, Cantu RC, Nowinski CJ, Hedley-Whyte ET, Gavett BE, Budson AE, et al. Chronic Traumatic Encephalopathy in Athletes. Journal of Neuropathology & Experimental Neurology. 2009; 68:709–735. [PubMed: 19535999]
7. Wennersten A, Meijer X, Holmin S, Wahlberg L, Mathiesen T. Proliferation, migration, and differentiation of human neural stem/progenitor cells after transplantation into a rat model of traumatic brain injury. Journal of Neurosurgery. 2004; 100:88–96. [PubMed: 14743917]
8. Harting MT, Sloan LAE, Jimenez F, Baumgartner J, Cox CS. Subacute Neural Stem Cell Therapy for Traumatic Brain Injury. Journal of Surgical Research. 2009; 153:188–194. [PubMed: 18694578]

9. Harting MT, Baumgartner JE, Worth LL, Ewing-Cobbs L, Gee AP, Day M-C, et al. Cell therapies for traumatic brain injury. Neurosurgical FOCUS. 2008; 24:E18. [PubMed: 18341394]
10. Riess P, Zhang C, Saatman KE, Laurer HL, Longhi LG, Raghupathi R, et al. Transplanted neural stem cells survive, differentiate, and improve neurological motor function after experimental traumatic brain injury. Neurosurgery. 2002; 51:1043–1054. [PubMed: 12234415]
11. Morganti-Kossmann MC, Rancan M, Otto VI, Stahel PF, Kossmann T. Role of cerebral inflammation after traumatic brain injury: a revisited concept. Shock. 2001; 16:165–177. [PubMed: 11531017]
12. Ziebell JM, Morganti-Kossmann MC. Involvement of Pro- and Anti-Inflammatory Cytokines and Chemokines in the Pathophysiology of Traumatic Brain Injury. Neurotherapeutics. 2010; 7:22–30. [PubMed: 20129494]
13. Hicks RR, Martin VB, Zhang L, Seroogy KB. Mild experimental brain injury differentially alters the expression of neurotrophin and neurotrophin receptor mRNAs in the hippocampus. Experimental Neurology. 1999; 160:469–478. [PubMed: 10619564]
14. Imitola J, Raddassi K, Park KI, Mueller F-J, Nieto M, Teng YD, et al. Directed migration of neural stem cells to sites of CNS injury by the stromal cell-derived factor 1α/CXC chemokine receptor 4 pathway. Proceedings of the National Academy of Sciences. 2004; 101:18117–18122.
15. Itoh T, Satou T, Ishida H, Nishida S, Tsubaki M, Hashimoto S, et al. The relationship between SDF-1 α/CXCR4 and neural stem cells appearing in damaged area after traumatic brain injury in rats. Neurological Research. 2009; 31:90–102. [PubMed: 19228460]
16. Bignami A, Hosley M, Dahl D. Hyaluronic acid and hyaluronic acid-binding proteins in brain extracellular matrix. Anatatomical Embryology (Berl). 1993; 188:419–433.
17. Bonneh-Barkay D, Wiley CA. Brain Extracellular Matrix in Neurodegeneration. Brain Pathology. 2009; 19:573–585. [PubMed: 18662234]
18. Lindwall C, Olsson M, Osman AM, Kuhn HG, Curtis MA. Selective expression of hyaluronan and receptor for hyaluronan mediated motility (Rhamm) in the adult mouse subventricular zone and rostral migratory stream and in ischemic cortex. Brain Research. 2013; 1503:62–77. [PubMed: 23391595]
19. Brännvall K, Bergman K, Wallenquist U, Svahn S, Bowden T, Hilborn J, et al. Enhanced neuronal differentiation in a three-dimensional collagen-hyaluronan matrix. Journal of Neuroscience Research. 2007; 85:2138–2146. [PubMed: 17520747]
20. Tian WM, Hou SP, Ma J, Zhang CL, Xu QY, Lee IS, et al. Hyaluronic acid-poly-D-lysine-based three-dimensional hydrogel for traumatic brain injury. Tissue Engineering. 2005; 11:513–525. [PubMed: 15869430]
21. Wei YT, Tian WM, Yu X, Cui FZ, Hou SP, Xu QY, et al. Hyaluronic acid hydrogels with IKVAV peptides for tissue repair and axonal regeneration in an injured rat brain. Biomedical Materials. 2007; 2:S142–S146. [PubMed: 18458459]
22. Wang Y, Wei YT, Zu ZH, Ju RK, Guo MY, Wang XM, et al. Combination of hyaluronic acid hydrogel scaffold and PLGA microspheres for supporting survival of neural stem cells. Pharmaceutical Research. 2011; 28:1406–1414. [PubMed: 21537876]
23. Lisignoli G, Cristino S, Piacentini A, Cavallo C, Caplan AI, Facchini A. Hyaluronan-based polymer scaffold modulates the expression of inflammatory and degradative factors in mesenchymal stem cells: Involvement of Cd44 and Cd54. Journal of Cellular Physiology. 2006; 207:364–373. [PubMed: 16331675]
24. Purcell BP, Elser JA, Mu A, Margulies KB, Burdick JA. Synergistic effects of SDF-1a chemokine and hyaluronic acid release from degradable hydrogels on directing bone marrow derived cell homing to the myocardium. Biomaterials. 2012; 33:7849–7857. [PubMed: 22835643]
25. Avigdor A. CD44 and hyaluronic acid cooperate with SDF-1 in the trafficking of human CD34+ stem/progenitor cells to bone marrow. Blood. 2004; 103:2981–2989. [PubMed: 15070674]
26. Naruse M, Shibasaki K, Yokoyama S, Kurachi M, Ishizaki Y. Dynamic Changes of CD44 Expression from Progenitors to Subpopulations of Astrocytes and Neurons in Developing Cerebellum. PLoS ONE. 2013; 8:e53109. [PubMed: 23308146]
27. Liu Y, Han SSW, Wu Y, Tuohy TMF, Xue H, Cai J, et al. CD44 expression identifies astrocyte-restricted precursor cells. Developmental Biology. 2004; 276:31–46. [PubMed: 15531362]

28. Shu XZ, Ghosh K, Liu Y, Palumbo FS, Luo Y, Clark RA, et al. Attachment and spreading of fibroblasts on an RGD peptide-modified injectable hyaluronan hydrogel. Journal of Biomedical Material Research. 2003; 68A:365–375.
29. Addington CP, Pauken CM, Caplan MR, Stabenfeldt SE. The role of SDF-1α-ECM crosstalk in determining neural stem cell fate. Biomaterials. 2014; 35:3263–3272. [PubMed: 24438907]
30. Vercruysse KP, Marecak DM, Marecek JF, Prestwich GD. Synthesis and in vitro degradation of new polyvalent hydrazide cross-linked hydrogels of hyaluronic acid. Bioconjugate Chemistry. 1997; 8:686–694. [PubMed: 9327132]
31. Shu XZ, Liu Y, Palumbo F, Prestwich GD. Disulfide-crosslinked hyaluronan-gelatin hydrogel films: a covalent mimic of the extracellular matrix for in vitro cell growth. Biomaterials. 2003; 24:3825–3834. [PubMed: 12818555]
32. Ellman GL. Tissue sulfhydryl groups. Archives of Biochemistry and Biophysics. 1959; 82:70–77. [PubMed: 13650640]
33. Heffernan JM, Overstreet DJ, Le LD, Vernon BL, Sirianni RW. Bioengineered Scaffolds for 3D Analysis of Glioblastoma Proliferation and Invasion. Annals of Biomedical Engineering. 2014
34. Azari H, Sharififar S, Rahman M, Ansari S, Reynolds BA. Establishing Embryonic Mouse Neural Stem Cell Culture Using the Neurosphere Assay. Journal of Visual Experiments. 2011:e2457.
35. Lu Y-B, Franze K, Seifert G, Steinhäuser C, Kirchhoff F, Wolburg H, et al. Viscoelastic properties of individual glial cells and neurons in the CNS. Proceedings of the National Academy of Sciences. 2006; 103:17759–17764.
36. Shu XZ, Ahmad S, Liu Y, Prestwich GD. Synthesis and evaluation of injectable, in situ crosslinkable synthetic extracellular matrices for tissue engineering. Journal of Biomedical Material Research. 2006; 79A:902–912.
37. Shear DA, Tate MC, Archer DR, Hoffman SW, Hulce VD, LaPlaca MC, et al. Neural progenitor cell transplants promote long-term functional recovery after traumatic brain injury. Brain Research. 2004; 1026:11–22. [PubMed: 15476693]
38. Shear DA, Tate CC, Tate MC, Archer DR, LaPlaca MC, Stein DG, et al. Stem cell survival and functional outcome after traumatic brain injury is dependent on transplant timing and location. Restorative Neurology and Neuroscience. 2011; 29:215–225. [PubMed: 21697596]
39. Tate CC, Shear DA, Tate MC, Archer DR, Stein DG, LaPlaca MC. Laminin and fibronectin scaffolds enhance neural stem cell transplantation into the injured brain. Journal of Tissue Engineering and Regenerative Medicine. 2009; 3:208–217. [PubMed: 19229887]
40. Guan J, Zhu Z, Zhao RC, Xiao Z, Wu C, Han Q, et al. Transplantation of human mesenchymal stem cells loaded on colalgen scaffolds for the treatment of traumatic brain injury in rats. Biomaterials. 2013; 34:5937–5946. [PubMed: 23664090]
41. Wang T-Y, Forsythe JS, Nisbet DR, Parish CL. Promoting engraftment of transplanted neural stem cells/progenitors using biofunctionalised electrospun scaffolds. Biomaterials. 2012; 33:9188–9197. [PubMed: 23022345]
42. Yu X, Chen D, Zhang Y, Wu X, Huang Z, Zhou H, et al. Overexpression of CXCR4 in mesenchymal stem cells promotes migration, neuroprotection and angiogenesis in a rat model of stroke. Journal of the Neurological Sciences. 2012; 316:141–149. [PubMed: 22280945]
43. Wang Z, Wang Y, Wang Z, Gutkind S, Wang Z, Wang F, et al. Engineered Mesenchymal Stem Cells with Enhanced Tropism and Paracrine Secretion of Cytokines and Growth Factors to Treat Traumatic Brain Injury. Stem Cells. 2014; 33:456–467. [PubMed: 25346537]
44. Lu D, Mahmood A, Qu C, Hong X, Kaplan D, Chopp M. Collagen scaffolds populated with human marrow stromal cells reduce lesion volume and improve functional outcome after traumatic brain injury. Neurosurgery. 2007; 61:596. [PubMed: 17881974]
45. Qu C, Mahmood A, Liu XS, Xiong Y, Wang L, Wu H, et al. The treatment of TBI with human marrow stromal cells impregnated into collagen scaffold: Functional outcome and gene expression profile. Brain Research. 2011; 1371:129–139. [PubMed: 21062621]
46. Suri S, Schmidt CE. Cell-laden hydrogel constructs of hyaluronic acid, collagen, and laminin for neural tissue engineering. Tissue Engineering Part A. 2010; 16:1703–1716. [PubMed: 20136524]

47. Tavazoie M, Van der Veken L, Silva-Vargas V, Louissaint M, Colonna L, Zaidi B, et al. A Specialized Vascular Niche for Adult Neural Stem Cells. Cell Stem Cell. 2008; 3:279–288. [PubMed: 18786415]
48. Kokovay E, Goderie S, Wang Y, Lotz S, Lin G, Sun Y, et al. Adult SVZ Lineage Cells Home to and Leave the Vascular Niche via Differential Responses to SDF1/CXCR4 Signaling. Cell Stem Cell. 2010; 7:163–173. [PubMed: 20682445]
49. Preston M, Sherman LS. Neural Stem Cell Niches: Critical Roles for the Hyaluronan-Based Extracellular Matrix in Neural Stem Cell Proliferation and Differentiation. Frontiers in Bioscience (Scholar Edition). 2012; 3:1165. [PubMed: 21622263]
50. Deboux C, Ladraa S, Cazaubon S, Ghribi-Mallah S, Weiss N, Chaverot N, et al. Overexpression of CD44 in Neural Precursor Cells Improves Trans-Endothelial Migration and Facilitates Their Invasion of Perivascular Tissues In Vivo. PLoS ONE. 2013; 8:e57430. [PubMed: 23468987]
51. Tran PB, Banisadr G, Ren D, Chenn A, Miller RJ. Chemokine receptor expression by neural progenitor cells in neurogenic regions of mouse brain. Journal of Computational Neurology. 2006; 500:1007–1034.
52. Cohen M, Kam Z, Addadi L, Geiger B. Dynamic study of the transition from hyaluronan- to integrin-mediated adhesion in chondrocytes. Embo Journal. 2006; 25:302–311. [PubMed: 16407968]
53. Lee JL, Wang MJ, Sudhir PR, Chen JY. CD44 Engagement Promotes Matrix-Derived Survival through the CD44-SRC-Integrin Axis in Lipid Rafts. Molecular and Cellular Biology. 2008; 28:5710–5723. [PubMed: 18644869]
54. Martino G, Pluchino S. The therapeutic potential of neural stem cells. Nature Reviews Neuroscience. 2006; 7:395–406. [PubMed: 16760919]
55. Turley EA, Noble PW, Bourguignon LYW. Signaling Properties of Hyaluronan Receptors. Journal of Biological Chemistry. 2002; 277:4589–4592. [PubMed: 11717317]
56. Wozniak MA, Modzelewska K, Kwong L, Keely PJ. Focal adhesion regulation of cell behavior. Biochimica Et Biophysica Acta - Molecular Cell Research. 2004; 1692:103–119.
57. Huang Y-S, Cheng C-Y, Chueh S-H, Hueng D-Y, Huang Y-F, Chu C-M, et al. Involvement of SHP2 in focal adhesion, migration and differentiation of neural stem cells. Brain and Development. 2012; 34:674–684. [PubMed: 22118986]
58. Kim M-S, Park M-J, Moon E-J, Kim S-J, Lee C-H, Yoo H, et al. Hyaluronic acid induces osteopontin via the phosphatidylinositol 3-kinase/Akt pathway to enhance the motility of human glioma cells. Cancer Research. 2005; 65:686–691. [PubMed: 15705860]
59. Rooney P, Wang M, Kumar P, Kumar S. Angiogenic oligosaccharides of hyaluronan enhance the production of collagens by endothelial cells. Journal of Cell Science. 1993; 105:213–218. [PubMed: 7689574]
60. Price J, Hynes RO. Astrocytes in culture synthesize and secrete a variant form of fibronectin. Journal of Neuroscience. 1985; 5:2205–2211. [PubMed: 3894594]
61. Jensen JB, Parmar M. Strengths and limitations of the neurosphere culture system. Molecular Neurobiology. 2006; 34:153–161. [PubMed: 17308349]
62. Suslov ON, Kukekov VG, Ignatova TN, Steindler DA. Neural stem cell heterogeneity demonstrated by molecular phenotyping of clonal neurospheres. Proceedings of the National Academy of Sciences. 2002; 99:14506–14511.
63. Wu PH, Giri A, Sun SX, Wirtz D. Three-dimensional cell migration does not follow a random walk. Proceedings of the National Academy of Sciences. 2014; 111:3949–3954.
64. Friedl P, Wolf K. Plasticity of cell migration: a multiscale tuning model. The Journal of Cell Biology. 2010; 188:11–19. [PubMed: 19951899]
65. Fraley SI, Feng Y, Krishnamurthy R, Kim D-H, Celedon A, Longmore GD, et al. A distinctive role for focal adhesion proteins in three- dimensional cell motility. Nature Publishing Group. 2010; 12:598–604.
66. Friedl P, Bröcker E-B. The biology of cell locomotion within three-dimensional extracellular matrix. Cellular and Molecular Life Sciences. 2000; 57:41–64. [PubMed: 10949580]

67. Jacques TS, Relvas JB, Nishimura S, Pytela R, Edwards GM, Streuli CH. Neural precursor cell chain migration and division are regulated through different beta1 integrins. Development. 1998; 125:3167–3177. [PubMed: 9671589]

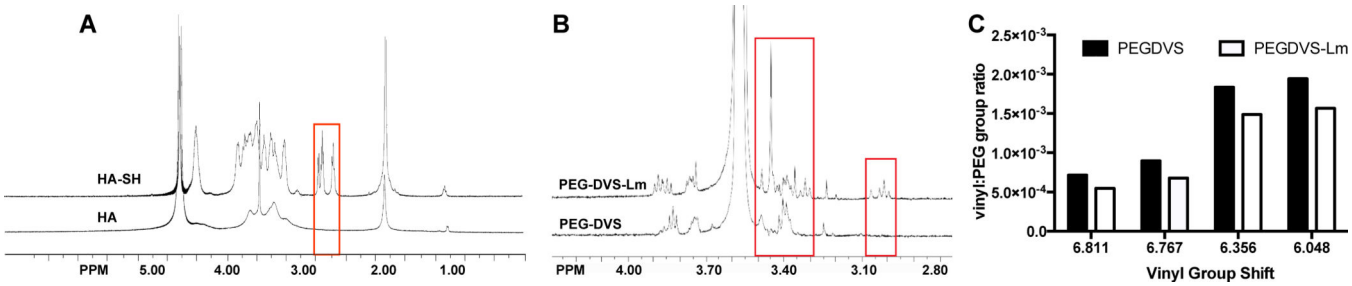

Figure 1.

Gel formulation proof of concept. Successful HA thiolation was evidenced by the appearance of thiol group peaks (red rectangle) in the NMR spectra of HA-S compared to HA (A). Laminin was covalently immobilized to PEGDVS as evidenced by the appearance of peptide peaks (red rectangles) in the NMR spectra of PEGDVS-Lm compared to PEGDVS (B). The PEGDVS-Lm spectra had a marked reduction in the ratio of free vinyl groups to PEG groups compared to PEGDVS (C), indicative of vinyl groups having bound to laminin free thiols.

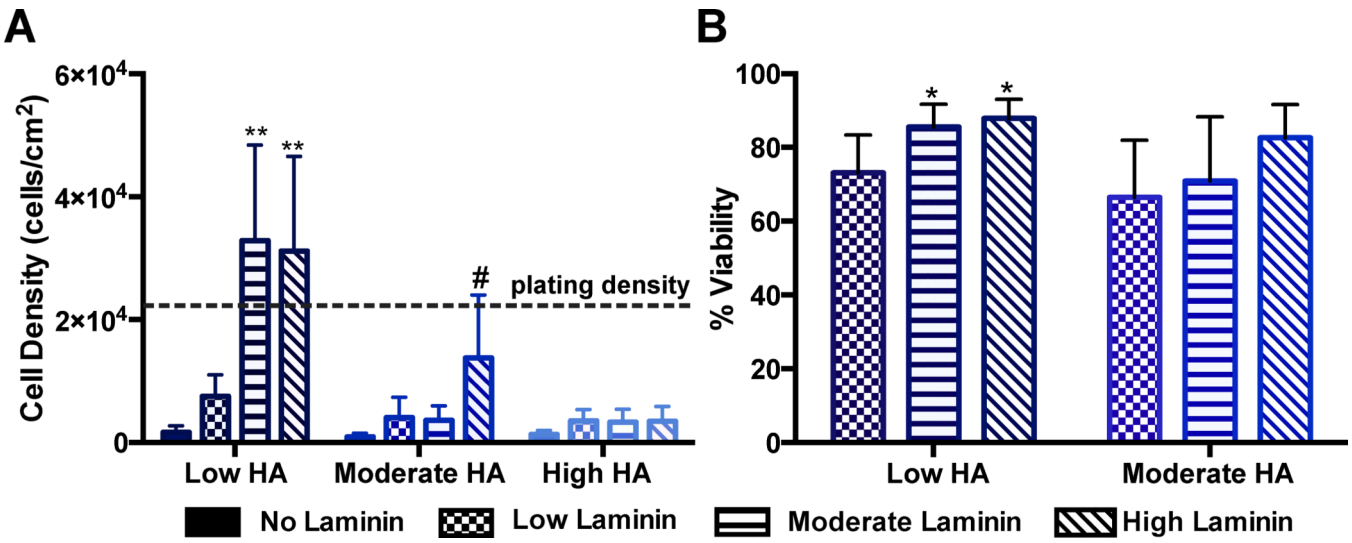

Figure 2.

NPSC density and viability after 72 hours of culture on a spectrum of gel formulations. NPSC density was significantly higher on gels with low HA and moderate and high Lm content compared to all other gels formulations and these were the only formulations in which density increased over the plating density (A). Moderate HA/High Lm supported significantly higher NPSC density than other moderate HA formulations, but it did not exceed the initial plating density. Low HA/Moderate and High Lm gels supported significantly higher NPSC viability compared to the Low HA/Low Lm gel and to the Moderate HA/Low and Moderate Lm gels (B). **$p<0.01$ compared to Low HA/No and Low Lm gel, all Moderate and High HA gels; #$p<0.05$ compared to other Moderate HA gels;*$p<0.05$ compared to all Low Lm gels and Moderate HA/Moderate Lm gel.

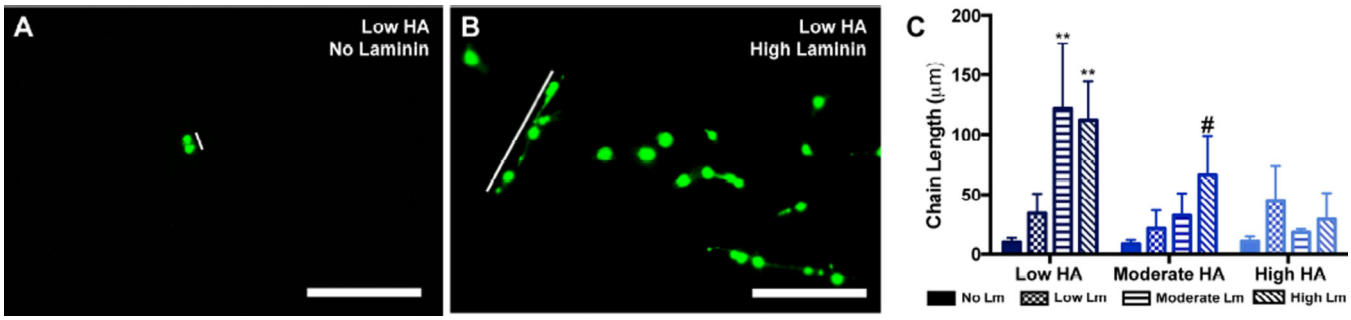

Figure 3.

NPSC chain length after 72 hours of culture on a spectrum of gel formulations. Chain length was measured in Matlab as a tertiary metric for gel optimization, where chainlike assemblies were defined as one or more NPSCs continuously connected via neurite outgrowth in a linear fashion (A,B). Chain length on low HA/Moderate and High Lm gels was significantly longer compared to all other gel formulations (C). Chain length on Moderate HA/High Lm gels was significantly longer than all other Moderate HA gels. **$p<0.01$ compared to Low HA/No and Low Lm gel, all Moderate and High HA gels; #$p<0.05$ compared to other Moderate HA gels. Scale bar is 100 microns.

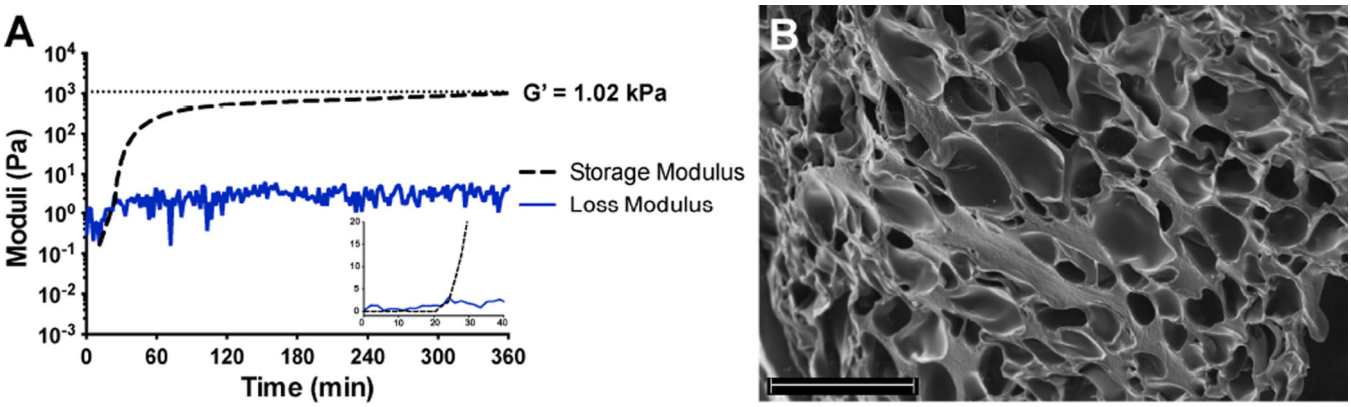

Figure 4.

Physical properties of the Low HA/Moderate Lm gel. HA-Lm gel storage modulus was 1.02 kPa, which is similar to that to native neural tissue (0.2–1.0 kPa) and gelation time was 24 minutes (A). SEM images illustrate that the microstructure is highly porous with interconnected pores ranging from 2–17 μm with an average aspect ratio of 2.12. Scale bar is 20 μm

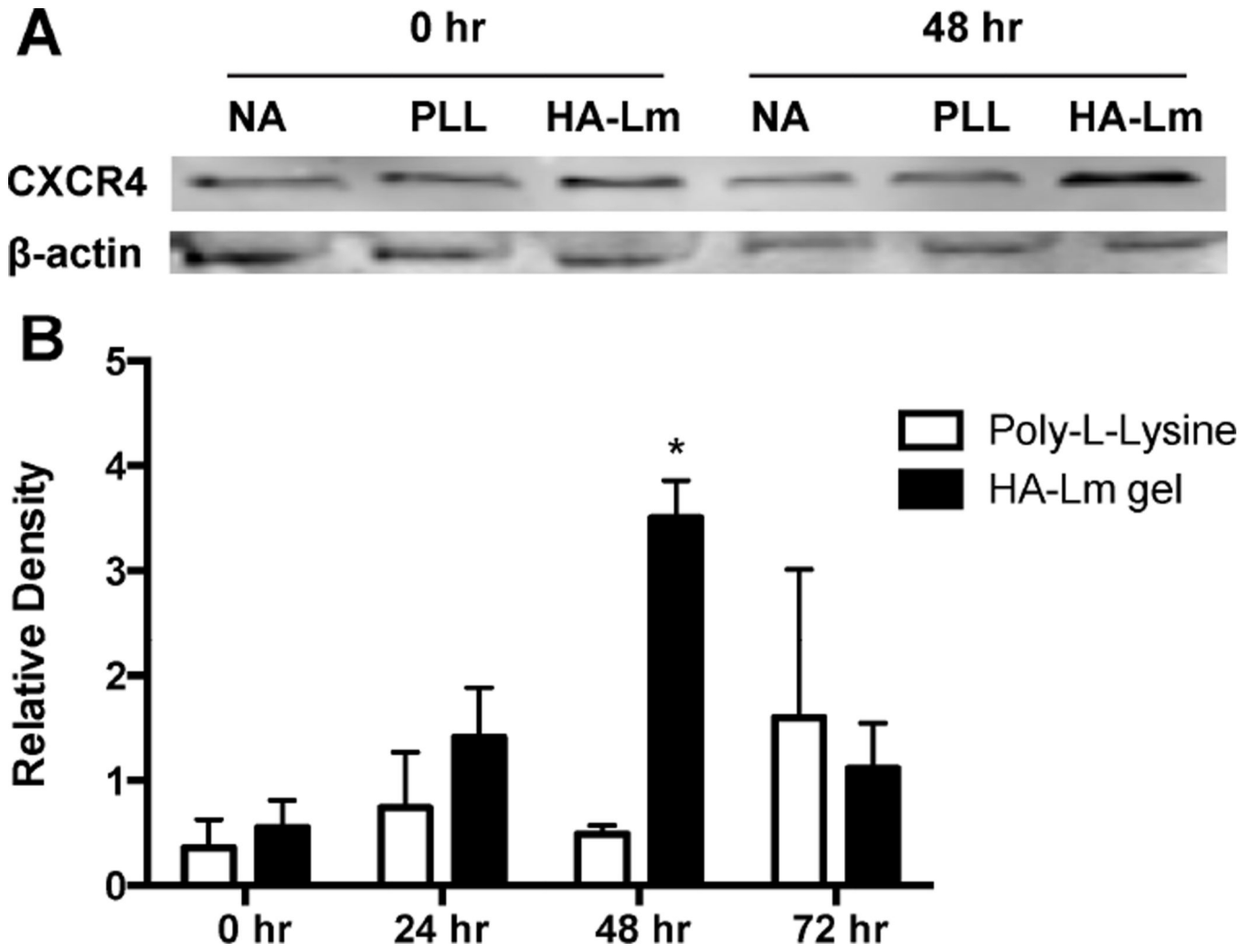

Figure 5.

HA-Lm gel promotes NPSC CXCR4 upregulation after 48 hours of culture. As determined by western blotting, NPSC CXCR4 protein expression on HA-Lm gel (Low HA/Moderate Lm) is significantly increased compared to PLL at all time points and to HA-Lm gel at all other times points (A,B). CXCR4 expression normalized internally to beta-actin expression and externally to CXCR4 expression in non-adherent culture (NA). *$p<0.05$ compared to all other time points and culture conditions.

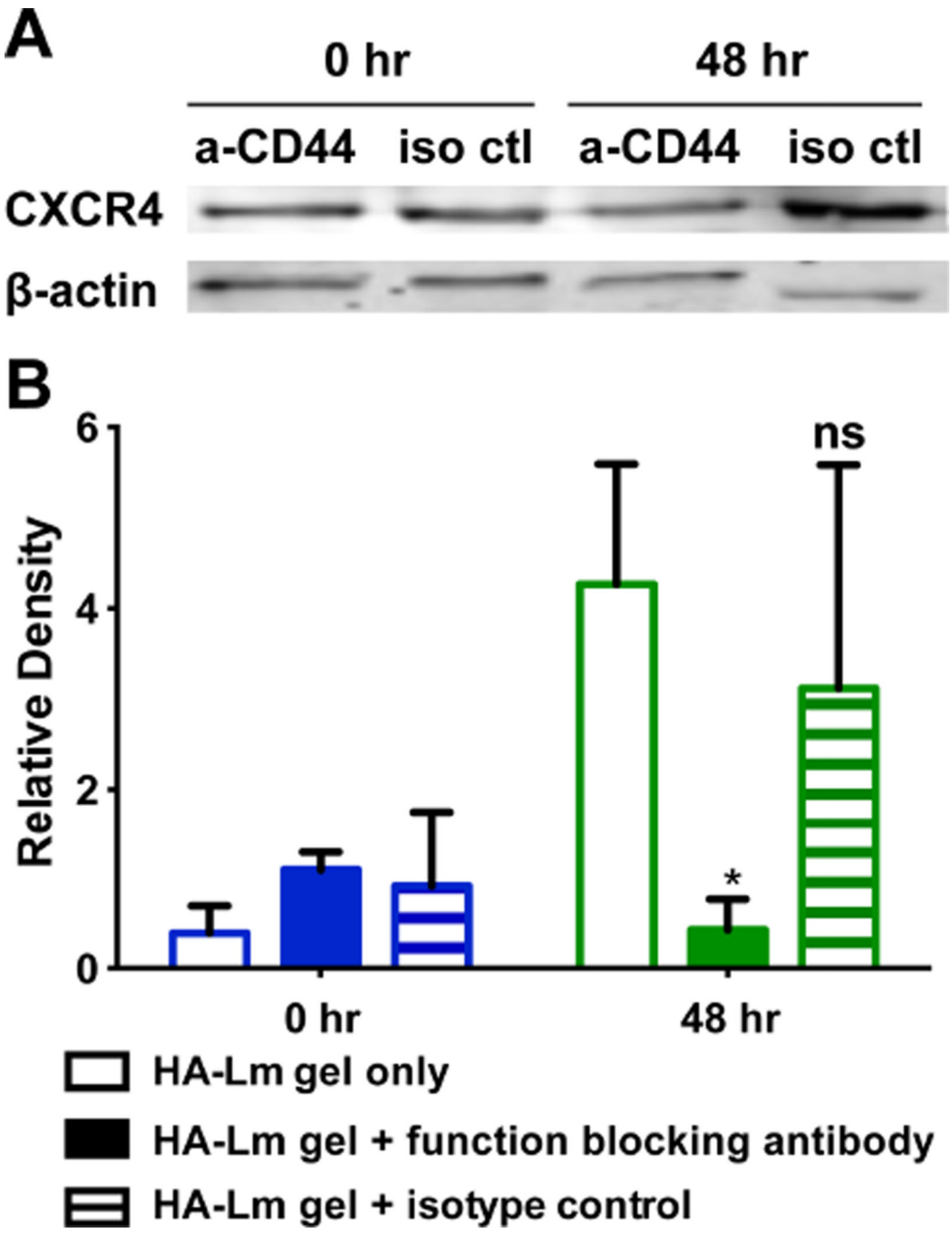

Figure 6.

HA-Lm gel-mediated NPSC CXCR4 upregulation is critically dependent on HA. Inhibition of HA with function blocking anti-CD44 abrogates CXCR4 upregulation at 48h (A,B). These differences were specifically due to HA inhibition as CXCR4 expression with isotype control supplementation was not significantly different from HA-Lm gel at 48h (B). Exclusion of Lm within the gel did not allow for sufficient adherence of NPSCs to the gel and thus protein levels were too low for effective detection by western blotting, leaving the

system irrelevant for transplantation. *$p<0.05$ compared to HA-Lm gel at 48 hr; ns = not significantly different from HA-Lm gel at 48 hr.

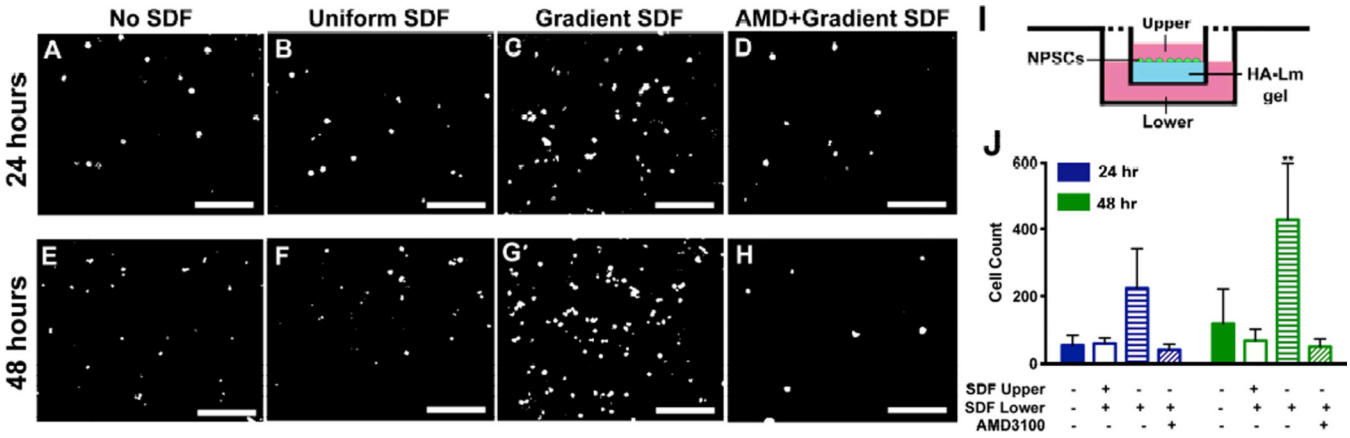

Figure 7.

HA-Lm gel supports NPSC chemotactic migration in response to SDF-1α gradients. NPSC migration within Transwell set up (I) is not significantly different in the absence of SDF-1α (A,E) compared to uniform SDF-1α concentration (B,F) at 24 and 48 h. In response to a SDF-1α gradient, NPSC migration increases at 24 h and significantly increases at 48 h compared to NPSCs not exposed to a SDF-1α gradient (J). This response is specifically mediated by SDF-1α as inhibiting its activity with AMD3100 reduced NPSC migration to levels observed in the absence of SDF-1α gradients. Scale bar is 150 microns, **p<0.01 compared to all other groups.

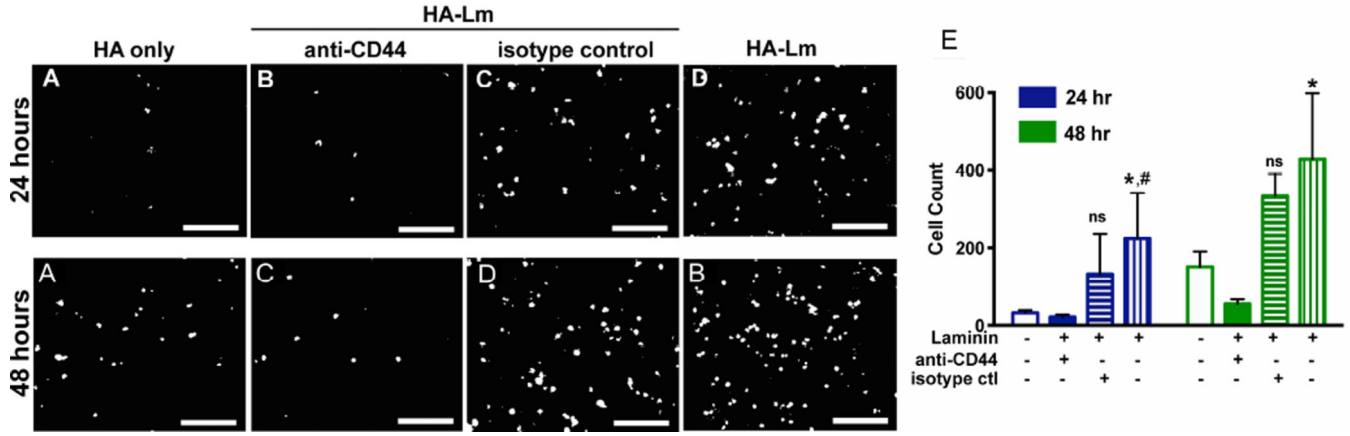

Figure 8.

NPSC chemotactic migration within HA-Lm gel is critically dependent on both HA and laminin. NPSC migration is significantly decreased on HA only gels compared to on HA-Lm gels at both 24 (A,D) and 48 hours (E,H). Moreover, NPSC migration is significantly decreased when HA signaling is inhibited with anti-CD44 at 24 (B) and 48 (F) hours compared to migration on HA-Lm gel (I). Reduced NPSC migration is due specifically to CD44 inhibition as the appropriate isotype control does not significantly affect NPSC migration. Scale bar is 150 microns, *$p<0.01$ compared to other groups of same time point, #$p<0.005$ compared to HA-Lm at 48 hours, ns = not significantly different from HA-Lm gel group of same time point.

Table 1

HA-Lm gel formulation naming convention. NPSC response was studied on all combinations of HA and laminin w/v percentages. Gel formulations will be referenced according to labels that provide relative descriptions of HA and laminin content. For example, a 1.75% HA/0.010% Lm gel will be referenced as a Low HA/Moderate Lm gel throughout the text.

Label	HA w/v	Laminin w/v%
No	N/A	0.000
Low	1.75	0.005
Moderate	2.00	0.010
High	2.25	0.015

Group	Gel	SDF-1α Exposure	Inhibitor Supplementation
1	HA-Lm	None	None
2	HA-Lm	Uniform	None
3	HA-Lm	Gradient	None
4	HA-Lm	Gradient	AMD3100
5	HA-Lm	Gradient	anti-CD44
6	HA-Lm	Gradient	anti-CD44 isotype control
7	HA only	Gradient	None